

A 10Gb/s GaAs PHEMT High Gain Preamplifier for Optical Receivers*

Jiao Shilong^{1,2,†}, Yang Xianming¹, Zhao Liang³, Li Hui³, Chen Zhenlong¹,
Chen Tangsheng^{2,3}, Shao Kai³, and Ye Yutang¹

(1 School of Optoelectronic Information, University of Electronic Science and Technology of China, Chengdu 610054, China)

(2 National Key Laboratory of Monolithic Integrated Circuits and Modules, Nanjing 210016, China)

(3 Nanjing Electronic Devices Institute, Nanjing 210016, China)

Abstract: A high gain cascade connected preamplifier for optical receivers is developed with 0.5 μ m GaAs PHEMT technology from the Nanjing Electronic Devices Institute. To begin with, the transimpedance amplifier has a -3dB bandwidth of 10GHz, with a small signal gain of around 9dB. The post-stage distributed amplifier (DA) has a -3dB bandwidth of close to 20GHz, with a small signal gain of around 12dB. As a whole, the cascade preamplifier has a measured small signal gain of 21.3dB and a transimpedance of 55.3dB Ω in a 50 Ω system. With a higher signal-to-noise ratio than that of the TIA and a markedly improved waveform distortion compared with that of the DA, the measured output eye diagram for 10Gb/s NRZ pseudorandom binary sequence is clear and symmetric.

Key words: GaAs PHEMT; optical receiver; preamplifier; eye diagram; cascade
EEACC: 1220

CLC number: TN722.3

Document code: A

Article ID: 0253-4177(2007)12-1902-10

1 Introduction

Optical receiver preamplifiers convert very weak input photocurrents into a preliminarily amplified voltage signal to avoid the submergence of the current signal into the larger noise current of a limiting amplifier (LA) due to the direct connection between a photodetector and the LA. Thus the preamplifier should have as low an equivalent input noise current as possible and a high transimpedance gain. Moreover, to meet the needs of high bit rate transmission, the preamplifier should also have a relatively large bandwidth^[1]. Unfortunately, these requirements conflict in general, and tradeoffs should be made according to practical targets.

Preamplifiers can be classified into lumped parameter amplifiers and distributed parameter amplifiers^[2]. The former, consisting of low impedance, high impedance, and transimpedance formats, has simpler topologies and flatter gain

curves. The transimpedance amplifier also pays attention to both the gain-bandwidth product and low noise performances through the tuning of a feedback resistance, so it is the most extensively used lumped amplifier. As for the distributed amplifier, it incorporates the input and output capacitances of transistors into artificial transmission line (ATL) structures to enlarge the bandwidth effectively, and has become widely used in recent years, especially in the field of broadband applications^[3~5]. The cascade configuration of TIA and DA make use of the advantages mentioned above, achieving a significant improvement of the small signal gain without a significant degradation of the bandwidth, which cannot be realized by conventional ways—enlarging the feedback resistance of TIA or the gate width of transistors for gain improvements. So the cascade amplifier benefits the sensitivity and bit error rate (BER) for the optical receiver.

In this work, we develop a cascade preamplifier for optical receivers based on the 0.5 μ m

* Project supported by the National Natural Science Foundation of China (No.60277008) and the National Key Laboratory of Monolithic Integrated Circuits and Modules Foundation of China (No.51491050105DZ0201)

† Corresponding author. Email: j_shilong@163.com

Received 8 June 2007, revised manuscript received 19 July 2007

©2007 Chinese Institute of Electronics

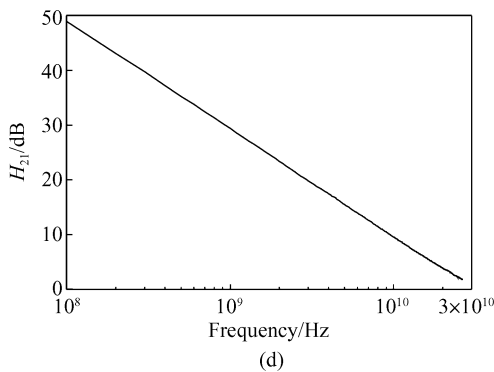
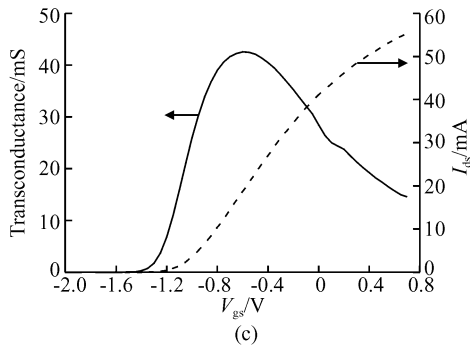
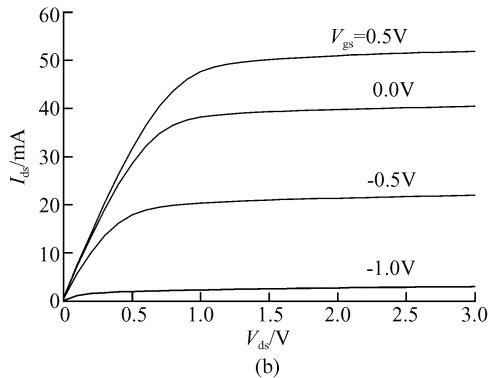
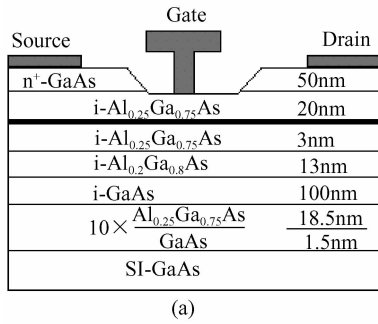


Fig. 1 (a) Cross section of PHEMT; (b) Output characteristic; (c) Transfer characteristic; (d) Forward current gain of H_{21}

GaAs PHEMT technology of the Nanjing Electronic Devices Institute, which consists of a fore-stage of TIA and a post-stage of DA. Results show

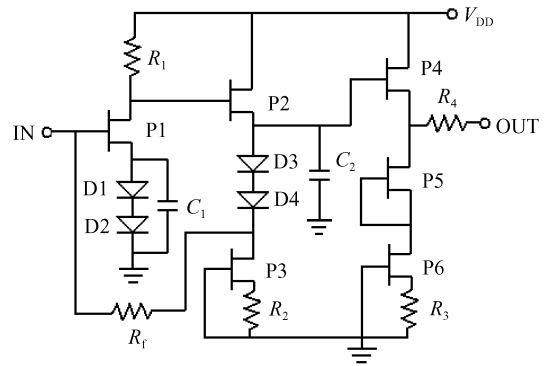


Fig. 2 Schematic of transimpedance amplifier

that the cascade preamplifier functions well at 10Gb/s.

2 Circuits design

2.1 PHEMT device

The active device of GaAs PHEMT, with the cross-section shown in Fig. 1(a), has a $0.5\mu\text{m}$ gate length and a $100\mu\text{m}$ gate width. The output characteristics and transfer characteristics are shown in Figs. 1 (b) and (c), respectively. The forward current gain curve of H_{21} , transformed from the on-wafer measured small signal S parameters under -0.8V gate-source and 1.5V drain-source biases, is shown in Fig. 1(d), from which we can see that the characteristic frequency is about 30GHz.

2.2 Transimpedance amplifier

The schematic of the transimpedance amplifier is shown in Fig. 2. The first stage is a common-source (CS) input unit with two Schottky diodes, D1 and D2, to elevate the source level for a negative gate-source bias of P1, while the shunt capacitance C_1 tends to reduce the negative feedback caused by D1 and D2 to improve the small signal gain, especially at high frequencies. The second and third stages are source followers used to realize level shifting and isolation between input and output ports. A feedback resistance R_f is placed between the source of P2 and the gate of P1 to form a voltage shunt negative feedback to stabilize gain and broaden bandwidth. Two Schottky diodes D3 and D4 are also adopted to reduce the source level of P2 for a proper minus bias of P1. To improve the gain shape and broaden the

bandwidth, a peaking capacitance C_2 is introduced between the two source followers. By the selection of R_2 and R_3 , the outputs of the two current sources P3 and P6 can be tuned, which is very important for P2 and P4 to get the proper biases in this single power supply scheme. Finally, the second source follower P4 should be selected deliberately, or else an extra resistance R_{out} has to be placed here for a good output standing wave ratio.

Under the conditions of single dominant pole assumption and without the influence of peaking capacitance C_2 , the -3dB bandwidth of TIA can be expressed as follows^[6,7]:

$$f_{-3\text{dB}} = \frac{A}{2\pi((C_g + AC_f)R_f + C_g R_g)} \quad (1)$$

And the transimpedance gain is:

$$Z_{\text{trans}} = \frac{-R_f}{1 + j2\pi f R_f \left(\frac{C_g}{A} + \frac{C_g R_g}{AR_f} + \frac{1}{j2\pi f R_f A} + C_f \right)} \quad (2)$$

where A is the open-loop gain, C_f and C_g are the parasitic capacitance of feedback resistance and gate capacitance of PHEMT, respectively, and R_g is the gate resistance of PHEMT.

From Eqs. (1) and (2), the increase of A will benefit the bandwidth and transimpedance gain, but there exists two restrictions: (1) The influence of Miller capacitance will become more and more significant with the increase of the open-loop gain, and even adversely affect bandwidth; (2) A certain phase margin is important to both the stability and a better pulse response of the amplifier. However, the increase of the open-loop gain may cause an extra transmission delay and phase shift. So a moderate A is desirable, especially at high bit rates.

The feedback resistance R_f plays an important role in bandwidth and transimpedance gains, as shown in Eqs. (1) and (2), as well as in the noise current shown in Eq. (7) in section 2.4. By the selection of R_f , these three parameters can be tuned easily. But, on the other hand, the variation directions of the three parameters with R_f are not the same, so tradeoffs should be made.

Furthermore, the capacitances of C_1 and C_2 have close relations to the small signal gain S_{21} and the bandwidth, as shown in Fig. 3(a); when $C_1 = 3\text{pF}$ and $C_2 = 0$, the solid S_{21} line, especially from median to high frequencies, is improved ef-

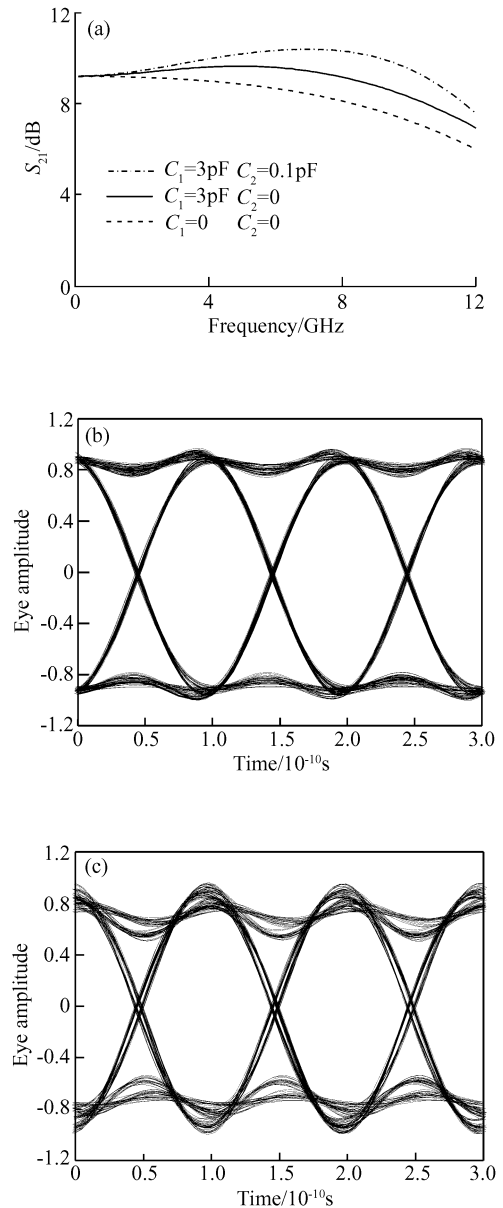


Fig.3 Influences of capacitances on gain, bandwidth and 10Gb/s output eye diagram of TIA (a) Small signal gain of S_{21} ; (b) Eye diagram with $C_1 = 3\text{pF}$, $C_2 = 0$; (c) Eye diagram with $C_1 = 3\text{pF}$, $C_2 = 0.2\text{pF}$

fectively compared with the dashed line, which is the result of $C_1 = 0$ and $C_2 = 0$; when $C_1 = 3\text{pF}$ and $C_2 = 0.1\text{pF}$, the S_{21} gets a certain peaking shown with the dashed-dotted line. In general, an overshoot less than 10% can be accepted in many applications^[8], because an over peaking effect may cause an over phase shifting, which will degrade the output eye diagram in the time domain and work against a high bit rate transmission, as shown in Figs. 3 (b) and (c).

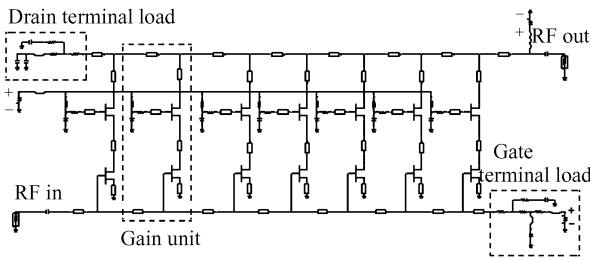


Fig.4 Schematic of distributed amplifier

2.3 Distributed amplifier

The schematic of a distributed amplifier is shown in Fig. 4, which consists of seven-stage cascode gain cells and two terminal loads. The periodic microstrips and the input impedance components of the cascode configuration construct a gate transmission line (gate-line), while the output microstrips and the output impedance components of the cascode configuration construct a drain transmission line (drain-line). When an input signal is fed to the gate terminals of the common-source PHEMTs, it is amplified by the transconductance and then travels to the drain-line. If only the phase velocities of the signals in the two transmission lines are roughly equal, the signals from each gain cell will add constructively at the output port^[3]. The residual signal in the gate-line and the reversely transmitting signal in the drain-line will be absorbed by the two terminal loads.

The cascode gain cell is the most important part of the distributed amplifier and is redrawn in Fig. 5 (a), where ML1~ML8 are microstrips, and F1 and F2 are common-gate and common-source PHEMTs, respectively. This cell is not only used for signal amplification, but also regarded as a loss compensation circuit which has a simplified equivalent scheme shown in Fig. 5 (b) with the output impedance^[9,10]:

$$Z_{out} = \frac{Z_{ds2} + j\omega(L_{ML5} + L_{ML6})}{\left(Z_{gs1} + R_2 + j\omega L_{ML4} + \frac{1}{j\omega C_1} \right) + [Z_{ds2} + j\omega(L_{ML5} + L_{ML6})]} \times \left[\frac{g_m Z_{ds1}}{j\omega C_{gs1}} + \left(Z_{gs1} + R_2 + j\omega L_{ML4} + \frac{1}{j\omega C_1} \right) \right] + Z_{ds1} \quad (3)$$

where 1 and 2 in the subscripts correspond to the PHEMT of F1 and F2, respectively, Z_{gs} is the gate-source impedance, and Z_{ds} is the drain-source impedance.

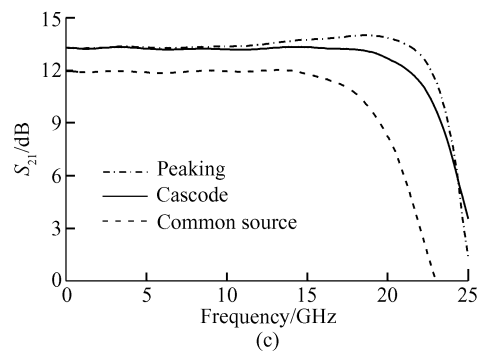
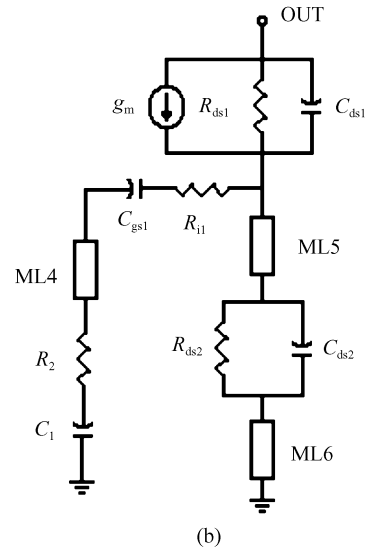
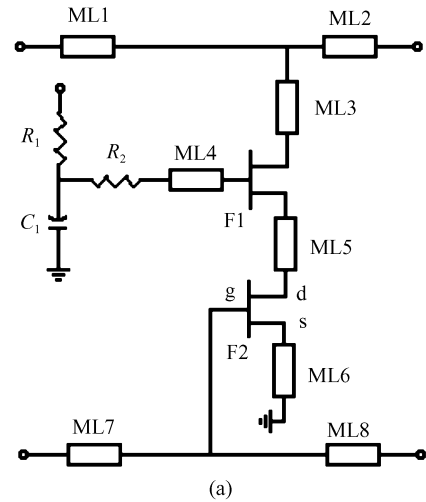


Fig.5 (a) Gain cell of DA; (b) Simplified loss compensation circuit; (c) Gain and bandwidth improvements

The real part of the first term on the right hand of Eq. (3) is negative under proper assignments, thus the drain-line loss can be compensa-

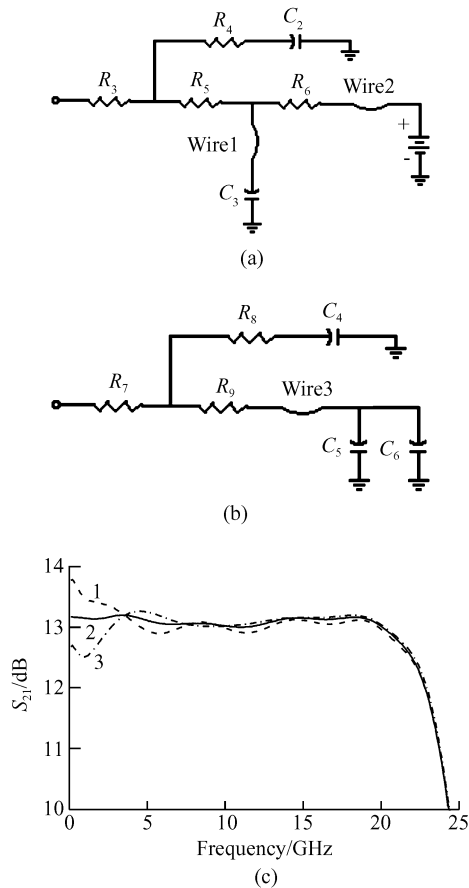


Fig.6 Transmission line loads and gain ripples (a) Load of the gate transmission line; (b) Load of the drain transmission line; (c) Influence of the gate-line load matching on the small signal gain of DA

ted, especially at high frequencies, resulting in significant improvements of gain and bandwidth, as shown in Fig. 5 (c); the dashed-dotted line and solid line are the simulated small signal gain curves with cascode gain cells, while the dashed line is the result of conventional DA topology with the same number of gain cells in which only a common-source PHEMT is used. The dashed-dotted line, with moderate gain peaking at high frequencies, also shows that the gain profile can easily be tuned through the selection of components C_1 , R_2 and ML3~ML6. Moreover, the negative resistance effect makes it possible for more gain cells to be added for even larger gain without compromising the bandwidth, because the number is actually limited by loss.

The terminal loads of gate-line and drain-line are shown in Figs.6 (a) and (b) respectively. Due to the much larger capacitance of the gate-line than that of the drain-line, the gate-line is more

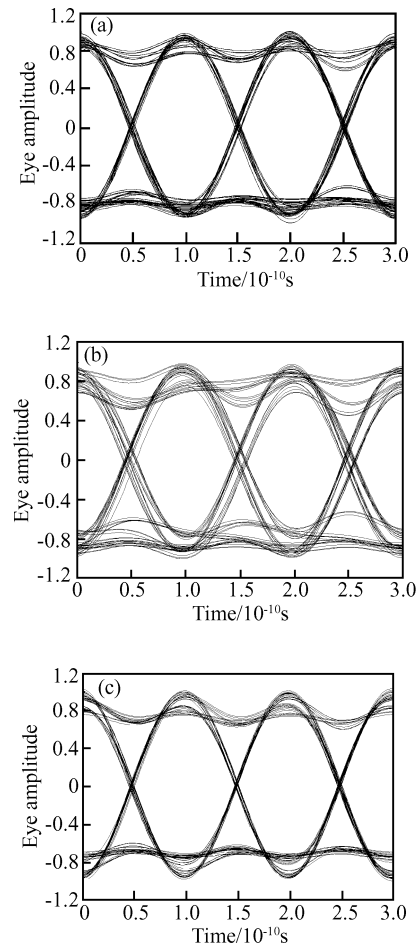


Fig. 7 Influences of impedance matching of gate transmission line terminal load on 10Gb/s output eye diagram of distributed amplifier (a) $R_3 = 15\Omega$; (b) $R_3 = 22\Omega$; (c) $R_3 = 8\Omega$

sensitive to signals, and any signal reflected from the terminal will lead to gain ripples, as shown in Fig. 6 (c); line 2 is the small signal gain under the condition that the terminal load, with $R_3 = 15\Omega$, has relatively good impedance matching with the gate-line; however, when $R_3 = 20$ or 10Ω , an overshoot or undershoot at low frequencies occurs as shown in line 1 or 3, as well as larger gain ripples at other frequencies. Thus, good impedance matching between the terminal loads and transmission lines should be realized for the absorption of redundant signals, and the key component R_3 should also be an alternative in view of process deviations, as shown in Fig. 8 (b), where three resistances are placed parallel at the terminals of the gate-line and the drain-line, respectively. In our design, there are two signal paths in each terminal load for signal absorption, while the gate-line load

also acts as a minus bias port.

To illustrate the influence of impedance mismatching on time domain performances, some 10Gb/s output eye diagrams of DA have been simulated as a function of the resistance R_3 . Results are shown in Fig. 7. When $R_3 = 22\Omega$, the “eyelid” becomes thicker, predicating a larger noise level and a reduced amplitude, and the timing jitter also increases markedly, as shown in Fig. 7 (b); when $R_3 = 8\Omega$, an obvious dumped ringing occurs, as shown in Fig. 7 (c). Thus, the impedance mismatching between the terminal loads and transmission lines degrade the output eye diagram of DA badly.

2.4 Noise analysis

There are four main noise sources in the transimpedance amplifier^[11]:

(1) Equivalent input Johnson noise current of common-source PHEMT:

$$\overline{i_j^2} = 4kT\Gamma \frac{(2\pi f C_g)}{g_m} \Delta f \quad (4)$$

(2) Shot noise current induced by the gate leakage current:

$$\overline{i_g^2} = 2qI_g \Delta f \quad (5)$$

(3) $1/f$ noise current:

$$\overline{i_{1/f}^2} = 4kT\Gamma \frac{(2\pi f C_g)^2}{g_m} \times \frac{f_c}{f} \Delta f \quad (6)$$

(4) Johnson noise current of the feedback resistance:

$$\overline{i_{R_f}^2} = \frac{4kT}{R_f} \Delta f \quad (7)$$

There are three main noise sources in the distributed amplifier^[12,13]:

(1) Noise current from the gate-line terminal load:

$$\overline{i_{gl}^2} = \frac{kT}{Z_{gl}} \left| 1 + \frac{Z_r}{Z_f} e^{jN\phi} \right| \quad (8)$$

(2) Noise current from the drain-line terminal load:

$$\overline{i_{dl}^2} = \frac{kT}{Z_{dl}} \left| \frac{Z_{dl}}{Z_f} \right|^2 \quad (9)$$

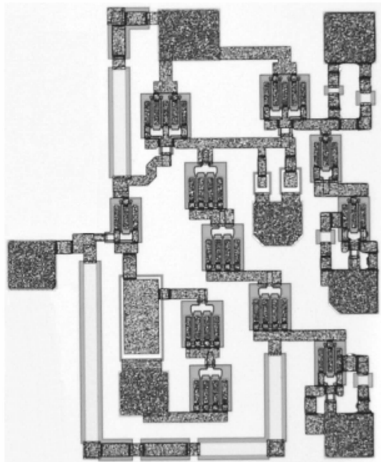
(3) Noise current from the cascode cells:

$$\overline{i_{cascode}^2} = \left| \sum_{k=1}^N \left(\frac{i_{gk}}{2D_g} \left(\frac{Z_{fk}}{Z_f} + \frac{Z_{rk}}{Z_f} + e^{-(k-\frac{1}{2})\theta_g} \right) + \frac{Z_{ld}}{Z_f} \times \frac{i_{dk}}{2D_d} e^{-(n-k+\frac{1}{2})\theta_d} \right) \right|^2 \quad (10)$$

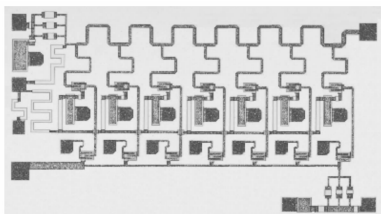
where k is the Boltzmann constant, T is the absolute temperature, Γ is the noise factor, Δf is the bandwidth, g_m is the transconductance of

PHEMT, C_g is the gate capacitance of PHEMT, q is the electron charge, I_g gate leakage current of PHEMT, f_c noise corner frequency of PHEMT, Z_f forward gain of DA, Z_r backward gain of DA, N gain cell number of DA, ϕ transmission delay, θ_g , θ_d propagation constants of gate-line and drain-line, respectively, i_{gk} , i_{dk} equivalent gate and drain noise current of the k th cascode cell, respectively, Z_{fk} , Z_{rk} forward and backward gain induced by the k th cascode cell, respectively, D_g , D_d current division terms at gate and drain, respectively, Z_{gl} , Z_{dl} impedance of the gate-line and the drain-line load, respectively, and Z_{ld} drain II-section image impedance of the m -derived section.

From these equations, we can see that the TIA has relatively simpler expressions for equivalent input noise current with explicit physical meaning, whereas the DA, with more complex equivalent circuit and noise model of cascode configuration, has noise current terms with a seemingly indirect relation to PHEMT's parameters. In fact, all the noise currents mentioned above come from three sources: (1) Noise from the PHEMT, which consists of Johnson noise, shot noise, and $1/f$ noise. The first two are coupled to the input and output terminals of the PHEMT by intrinsic capacitances. At the input, the noise current is converted into noise voltage due to the input impedance of the PHEMT, and it is amplified by the transconductance, forming the output noise voltage together with the noise formerly coupled to the output terminal. These capacitive coupling effects become more significant with the increase of frequency, thus the noise augments rapidly, which is also the fundamental reason for the conclusion emphasized in Ref. [13] that the output noise of the cascode cell is the most significant contributor to the total noise of the DA especially at high frequencies, as well as that the contribution of transistor loss to the total noise should not be ignored. So a transistor for low noise applications should have the characteristics such as low intrinsic capacitances and resistances, which also benefit the $1/f$ noise as shown in Eq. (6). Based on the facts mentioned above, a $0.5\mu\text{m}$ T-gate GaAs PHEMT is adopted in our design. (2) Noise from the feedback resistance, as shown in Eqs. (1) and (7), a large feedback resistance will reduce the Johnson noise, but there exists a limit of band-



(a)



(b)

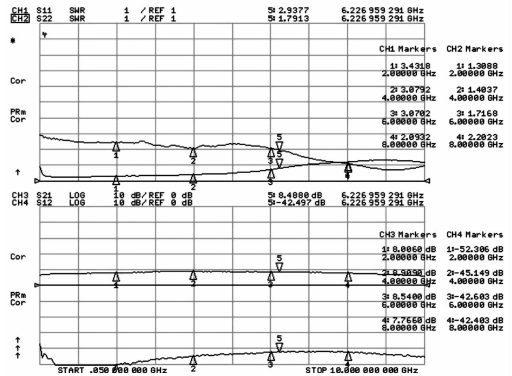


(c)

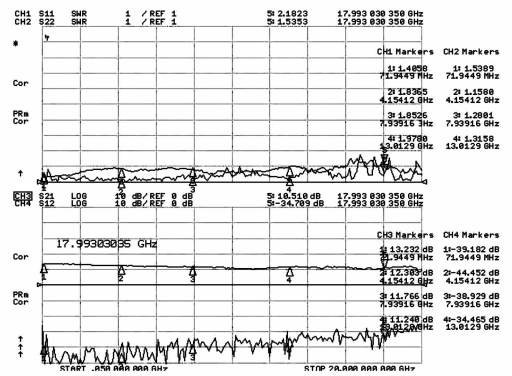
Fig.8 (a)Transimpedance amplifier die;(b)Distributed amplifier die;(c)Assembly for measurement

width. (3) Noise from the terminal loads of transmission lines, as shown in Eqs. (8) and (9), a large impedance will reduce the noise current effectively, and reports show that the equivalent input noise current spectrum density of DA is reduced 25% only by the enlargement of gate-line load impedance from 50 to 100Ω^[12]. However, for meeting the impedance matching condition, the gate-line characteristic impedance will also be enlarged, resulting in a decrease in the cut-off frequency, thus the bandwidth is reduced.

From the above discussion, we see that the transistor parameters, such as capacitance, resistance, and transconductance are crucial to the noise performances of TIA and DA, so the selection of an active device is the primary task in the



(a)



(b)

Fig.9 (a)Small signal S parameter of TIA;(b)Small signal S parameter of DA

design of a low noise amplifier. Furthermore, for some special qualifications, the circuit parameters, such as operating points, feedback resistance, gain cell and so on, may be tuned.

3 Measurements and performances

The TIA and DA dies, with areas of 1050μm × 1080μm and 2700μm × 1560μm, respectively, are fabricated on the Φ76mm GaAs PHEMT processing line of the Nanjing Electronic Device Institute, as shown in Figs. 8 (a) and (b). Before measurement, the dies were assembled into a special package which has microstrips bonded on the bottom and two SMA connectors terminating the ends, as shown in Fig. 8 (c). For TIA or DA alone, the input and output ports of the die are connected to the microstrips through golden wires, as to the cascade configuration of the two amplifiers, the output of the TIA and the input of the DA are connected together through a microstrip and golden wires. The biases, fed through the

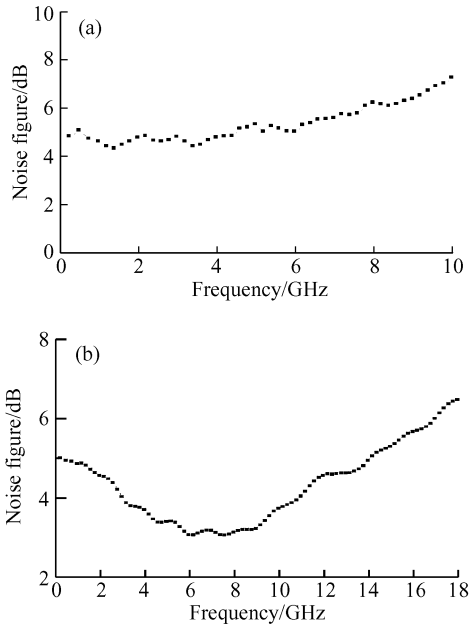
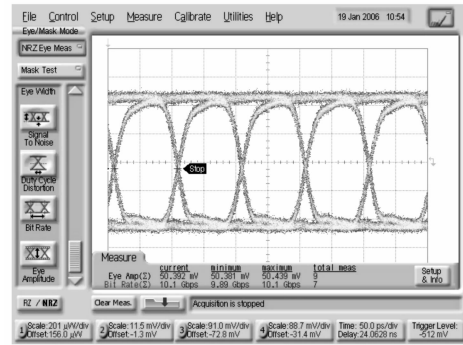


Fig. 10 (a) Noise figure of TIA; (b) Noise figure of DA

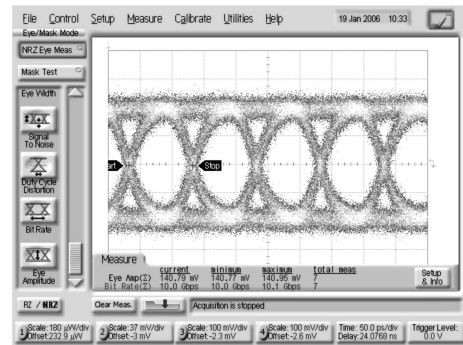
needles on both sides of the package, are 5V (60mA), 3.5V (100mA) and -0.8V for the TIA and DA, respectively.

The small signal S parameters of the TIA and DA were measured under -30dBm input power with an Agilent 8720ES vector network analyzer (VNA), and the results are shown in Figs. 9 (a) and (b). The TIA has a bandwidth of 10GHz, with a flat gain curve of S_{21} around 9dB from 2 to 8GHz, and the input standing wave ratio (SWR) is somewhat degraded since the selection of the common-source PHEMT and the feedback resistance emphasized gain and bandwidth. The DA has a bandwidth close to 20 Hz with a gain of around 12dB, and the input and output SWRs are less than 2. Both amplifiers have very good reverse isolations.

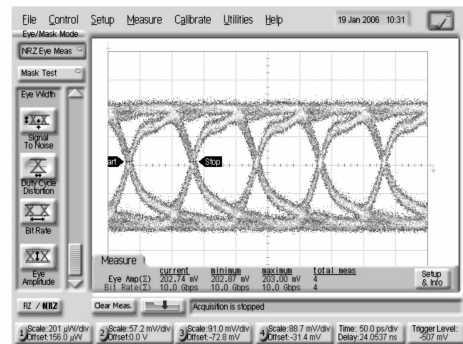
The noise figures (NF) were measured with an Agilent N8975A noise figure analyzer and the results are shown in Fig. 10. For the TIA, the NF varies in the range of 4.3~7.2dB with an average of 5.3dB, and, above 1.5GHz, the NF becomes larger with the increase of frequency in general. While the DA has an NF of 3~6.5dB with an average of 4.28dB, and the NF curve varies in two reverse tendencies with frequency on both sides of 7.5GHz, although there is a relatively flat bottom between 6~9GHz, so it looks like a saddle. The relation between the equivalent input noise cur-



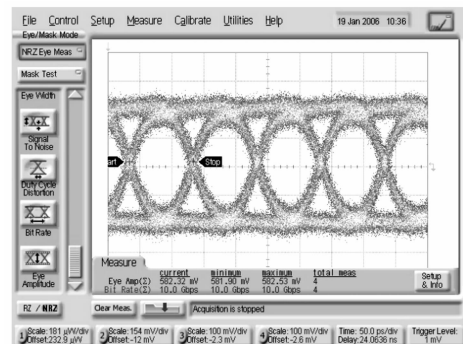
(a)



(b)



(c)



(d)

Fig. 11 10Gb/s eye diagram measurements of amplifiers (a) Eye diagram of input signal; (b) Output of TIA; (c) Output of DA; (d) Output of the cascade connection amplifier

rent and the noise figure is approximately^[9,14]:

$$\overline{i_{\text{eq}}^2} = \frac{4kT(10^{\text{NF}/20} - 1)\Delta f}{Z_0} \quad (11)$$

so the equivalent input noise current spectral densities of the TIA and DA are 16.7 and 14.6 pA/ $\sqrt{\text{Hz}}$, respectively.

To evaluate the time performances, we measured output eye diagrams using an ADVANTEST D3186 pulse pattern generator and an Agilent 86100A oscilloscope. The input signal was 10Gb/s NRZ pseudorandom binary sequences with a peak-to-peak amplitude of 50mV, as shown in Fig. 11 (a). In the output eye diagrams of Figs. 11 (b) and (c), the amplitude, timing jitter and signal-to-noise voltage ratio for TIA and DA are 140 and 202mV, 18 and 12ps, 3.4 and 8.8, respectively. The cascade configuration of TIA and DA has a symmetrical eye diagram with an amplitude of 582mV, which can be converted into a small signal gain of 21.3dB or a transimpedance gain of 55.3dB Ω in 50 Ω system, and the timing jitter and signal-to-noise voltage ratio are 17ps and 5.4, respectively, as shown in Fig. 11 (d). We can see that the cascade amplifier has a significantly enlarged gain and an improved signal-to-noise voltage ratio compared to that of TIA, which will benefit the sensitivity and bit error rate (BER) for the optical receiver. Moreover, the distortion of the input signal, amplified by the DA as shown in Fig. 11 (c), is also rectified by the cascade amplifier, as shown in Fig. 11 (d).

4 Conclusions

A cascade connected preamplifier is developed with domestic material and process technologies, which consists of two widely different amplifiers of TIA and DA. The influences of some key parameters on the performances, such as small signal gain, bandwidth, noise, and eye diagram are discussed in detail. The measurements show that not only do the TIA and DA perform well, but also that the cascade amplifier has a significantly enlarged gain, an improved signal-to-noise ratio,

as well as a good 10Gb/s functional mode.

Acknowledgements The author would like to thank Prof. Zeng Yiping and Wang Baoqiang for the epitaxial growth of PHEMT material.

References

- [1] Shibata T, Kimura S, Kimura H, et al. A design technique for a 60GHz-bandwidth distributed baseband amplifier IC module. *IEEE J Solid-State Circuits*, 1994, 29(12):1537
- [2] Alexander S B. *Optical communication receiver design*. Washington: SPIE, 1997
- [3] Robertson D, Lucyszyn S. *RFIC and MMIC design and technology*. London: The Institute of Electrical Engineers, 2001
- [4] Aguirre J, Plett C. 50-GHz SiGe HBT distributed amplifiers employing constant- k and m -derived filter sections. *IEEE Trans Microw Theory Tech*, 2004, 52(5):1573
- [5] Leich M, Hurm V, Sohn J, et al. 65GHz bandwidth optical receiver combining a flip-chip mounted waveguide photodiode and GaAs-based HEMT distributed amplifier. *Electron Lett*, 2002, 38(25):1706
- [6] Miyashita M, Maemura K, Yamamoto K, et al. An ultra broadband GaAs MESFET preamplifier IC for a 10Gb/s optical communication system. *IEEE Trans Microw Theory Tech*, 1992, 40(12):2439
- [7] Pedrotti K. High speed circuits for lightwave communications. *International Journal of High Speed Electronics and Systems*, 1998, 9(2):313
- [8] Abraham M. Design of butterworth-type transimpedance and bootstrap-transimpedance pre-amplifiers for fiber-optic receivers. *IEEE Trans Circuits Syst*, 1982, CAS-29(6):375
- [9] Jiao Shilong, Chen Tangsheng, Jiang Youquan, et al. 20GHz broadband GaAs PHEMT distributed preamplifier. *Acta Electronica Sinica*, 2007, 35(5):955 (in Chinese) [焦世龙, 陈堂胜, 蒋幼泉, 等. 20GHz 宽带 GaAs PHEMT 分布式前置放大器. *电子学报*, 2007, 35(5):955]
- [10] Kimura S, Imai Y, Umeda Y, et al. A 16-dB DC-to-50-GHz InAlAs/InGaAs HEMT distributed baseband amplifier using a new loss compensation technique. *IEEE GaAs IC Symposium*, 1994:96
- [11] Miyashita M, Maemura K, Yamamoto K, et al. An ultra broadband GaAs MESFET preamplifier IC for a 10Gb/s optical communication system. *IEEE Trans Microw Theory Tech*, 1992, 40(12):2439
- [12] Freundorfer A P, Nguyen T L. Noise in distributed MESFET amplifiers. *IEEE J Solid-State Circuits*, 1996, 31(8):1100
- [13] Ko W, Kwon Y. Improved noise analysis of distributed pre-amplifier with cascode FET cells. *IEEE Trans Microw Theory Tech*, 2005, 53(1):361
- [14] Park M S, Minasian R A. Ultra-low-noise and wideband-tuned optical receiver synthesis and design. *IEEE J Lightwave Technol*, 1994, 12(2):254

10Gb/s GaAs PHEMT 高增益光接收机前置放大器*

焦世龙^{1,2,†} 杨先明¹ 赵亮³ 李辉³ 陈镇龙¹ 陈堂胜^{2,3} 邵凯³ 叶玉堂¹

(1 电子科技大学光电信息学院, 成都 610054)

(2 单片集成电路与模块国家级重点实验室, 南京 210016)

(3 南京电子器件研究所, 南京 210016)

摘要: 基于南京电子器件研究所 0.5 μm GaAs PHEMT 工艺, 研制了一种高增益级联式光接收机前置放大器. 作为前级的跨阻抗放大器的 -3dB 带宽为 10GHz, 小信号增益为 9dB; 作为后级的分布式放大器的 -3dB 带宽接近 20GHz, 小信号增益为 12dB; 级联前置放大器小信号增益达 21.3dB, 跨阻增益为 55.3dB Ω , 在输入 10Gb/s 非归零伪随机二进制序列下, 放大器输出眼图清晰、对称、信噪比优于跨阻放大器, 分布放大器不能校正的输入波形失真也得到显著改善.

关键词: GaAs PHEMT; 光接收机; 前置放大器; 眼图; 级联

EEACC: 1220

中图分类号: TN722.3

文献标识码: A

文章编号: 0253-4177(2007)12-1902-10

* 国家自然科学基金(批准号:60277008)及单片集成电路与模块国家级重点实验室基金(批准号:51491050105DZ0201)资助项目

† 通信作者, Email: j_shilong@163.com

2007-06-08 收到, 2007-07-19 定稿